

## Aerodynamic Optimization In the Rotor of Centrifugal Fan Using Combined Laser Doppler Anemometry and CFD Modeling

*Javad Alinejad and Farhad Hosseinnnejad*

Department of Mechanical Engineering Sari Branch,  
Islamic Azad University, Sari, Iran

**Abstract:** The fan under consideration is forward-curved centrifugal fan used in an air-conditioner in order to investigate an integrated scheme, consisting of shape optimization, experimental verification and numerical simulation. The targeted topic in this particular study is the design optimization of a centrifugal fan in order to improve efficiency and rectify the non-uniformity of the flow and to eliminate the vortices that are generated by the existence of inlet distortion. Two types of rotor were used by different geometries in the current study: cylindrical and conical frustum-shaped. Numerical simulation was performed by a 3D turbulent, steady-state, incompressible flow analysis. The overall experiments were conducted in a standard ISO 5801:1997 test chamber apparatus. To obtain the occurring flow patterns inside the test section from the experimental data, the optical measurement technique Laser Doppler Anemometry (LDA) is applied in the analysis and they were used to validate the CFD simulations. The comparison of the results presented a great dependence of the rotor shape and the fan efficiency. Accordingly, the results indicate that, a conical frustum-shaped rotor with the optimal cone angle can cause a higher efficiency and performance than a cylindrical design at the similar conditions. Furthermore, the findings have revealed velocity components and a jet-wake pattern at the rotor outlet. The simulations were performed at realistic conditions and the numerical results agree well with the experiments.

**Key words:** Centrifugal fan • CFD • Efficiency • LDA • Rotor • Fluctuation

### INTRODUCTION

Forward-curved centrifugal fans have been widely used in industry. They are used as circulating fans in central heating and air-conditioning systems in buildings, as blowers in automotive heating/cooling units and in numerous other applications for their high capacity of mass flow, size compactness relatively high volumetric flow rates and a high pressure rise. Fans of this type are generally designed to use a large number of forward-curved blades and have a large inlet-exit diameter ratio and a relatively large rotor width which, both are their key distinguishing features. Thus, the resulting flow inside the fan has complex three-dimensional characteristics. The rotor is the principal part for a centrifugal fan and has significant effect on the performance outcome. The rotor is the major working surface for energy transfer and identified as having a great potential for improvement. Therefore, a conical frustum-shaped rotor is selected as the basic scheme in this study. Earlier researchers have

attempted to identify the general flow pattern inside the fan. In the early 1980's, Raj and Swim [1] studied the flow at the exit of a forward-curved (FC) centrifugal fan rotor using the smoke technique and hot wire probes. Their work presented the inactive region at the shroud end of the rotor, the jet-wake velocity profile at the blade exit and the separated flow at the leading edge of the blade suction surface. Moreover, the flow through the rotor was found to be highly turbulent and strongly three-dimensional, which was a function of the axial location on the rotor, the tangential position in the housing and the through flow rate. In the experimental work of Yamazaki and Satoh [2], the main through-flow was near the back plate of the rotor extending for about one fourth of the rotor's width at the inlet and two thirds of its width at the exit, while the remaining rotor span had little through-flow. Later, Kind and Tobin [3] implemented a five-hole probe technique to measure the mean flow field at the rotor inlet and exit, which indicated the presence of a flow reversal through the rotor blade. Thanks to particle tracing

velocimetry (PTV), Denger and McBride [4] reported a highly turbulent flow in the vicinity of the volute tongue. Kadota *et al.* [5] and Kawaguchi *et al.* [6] visualized the internal flow field using a spark tracing method and measured the pressure fluctuation on the blade surfaces with a semiconductor-type pressure sensor. They also found a highly complex flow pattern inside the fan and large pressure fluctuation on the blade surfaces near the shroud side of the rotor, as well as passing the volute tongue. Recently, Sandra *et al.* [7] have analyzed the velocity unsteadiness distribution at the rotor outlet with the hot wire technique. They have demonstrated that the unsteady characteristics of the flow are mainly determined by the flow rate and the circumferential position. Basing on these results, many researchers have attempted novel approaches and performed extensive (and partly successful) experiments [8–12] to predict and further improve the fan's performance. However, most of the research on this type of fans has been experimental. Computational and experimental methods may be employed to assess the performance of fans. The use of Computational Fluid Dynamics (CFD) for turbo machinery flows has significantly increased in the past years. Detailed CFD studies of the internal flow field of integral multi-blade centrifugal fan systems have been relatively limited. A CFD study can reduce the testing time and the related expense and avoid disturbance of the internal flow field of the fan by the test apparatus. Moreover, detailed information on the flow field can be obtained and the flow pattern throughout the fan can be visualized, thus enhancing our understanding of the complex flow physics inside the fan and offering guidance for fan design. Therefore, the objective of this study is to visualize the main flow phenomena occurring in a centrifugal fan, using experimental measurement technique Laser Doppler Anemometer. The overall behavior of the fan has been validated experimentally according to the ISO 5801:1997 standard. Also, this paper presents an internal flow field of a multi-blade centrifugal fan used in a household air-conditioner carried out with the FLUENT commercial CFD code. It covers the whole fan system, including the inlet, the rotor and the volute and presents a detailed analysis on the flow characteristics inside the fan, emphasized by the flow behavior in conical frustum-shaped rotor. The main objective of this work, is to assess the shape optimization on the fan performance. For this purpose, two different types of rotor are considered. The preference of a conical frustum-shaped rotor in delivering uniform distribution of air flow and have higher efficiency was demonstrated by performance comparisons.

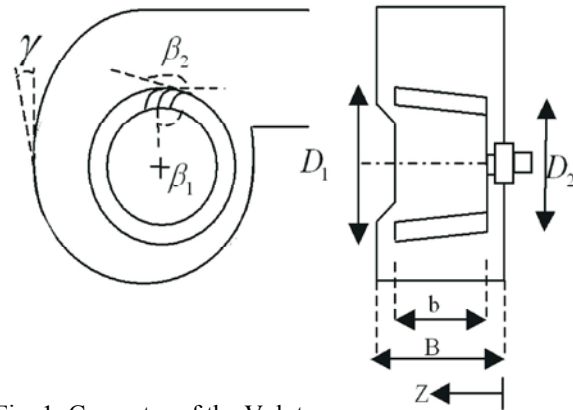


Fig. 1: Geometry of the Volute

Table 1: Rotor and Volute characteristics

Revolutions per Minute N (rpm)	745±1.8%
Number of Blades n	43
Volute Width B (mm)	200
Rotor Width b (mm)	165
Volute Expansion radius r (mm)	210
Outlet Diameter of Rotor1 D₂ (mm)	365
Outlet Diameter of Rotor2 D₂ (mm)	335
Inlet Diameter of Rotor1 D₂ (mm)	335
Inlet Diameter of Rotor2 D₁ (mm)	365
Volute Expansion Angle γ	5°
Inlet Angle β₁	90°
Outlet Angle β₂	155°

**CFD Modeling:** The geometry of the volute and rotor is shown in Fig. 1. The basic geometrical specification and operating conditions of fan and rotor are tabulated in Table 1. The fan consists of an inlet section, a rotor of 43 equally spaced straight blades and a volute. It should be noted that the rotor of tested fan has been designed conical frustum-shaped, but has a very small blade retaining shroud attached to the outer diameter of the blades.

A fully implicit, segregated finite volume method solving three-dimensional Reynolds-averaged Navier-Stokes viscous partial differential equations have been used in our numerical calculation to study the turbulent flow field of the multi-blade centrifugal fan. The standard two-equation  $k$ - $\epsilon$  turbulent model with standard wall functions has been applied to model the turbulent flow. The second-order upwind deference scheme has been employed to spatially discretize the convection terms. We use SIMPLE solution method in order to solve a system of coupled equations. The convergence criterion is set to be  $10^{-4}$  for the residual numbers.

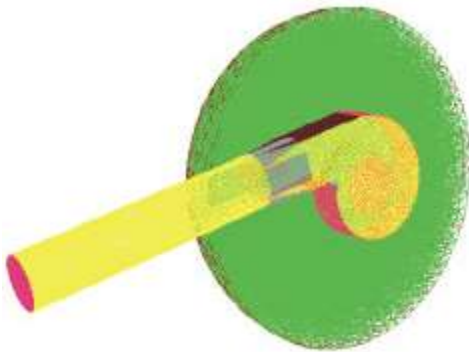


Fig. 2: Conical frustum-shaped rotor, volute, outlet region and hemispherical inlet region in isometric views

Numerical simulation based on the finite-volume numerical method using the FLUENT 6.2 software [13] has been carried out to consider the steady interactions between the rotating rotor blades and the stationary fan casing and to understand the internal flow. The geometrical parameters given in Table 1 have been used in order to generate the computational domain which has been divided into two zones, a rotational zone including the rotor and stationary zones elsewhere. This configuration takes into account the clearance between the rotor and the volute.

Therefore, the inlet and outlet surfaces of the fan have been extended in order to ensure numerical stability and to minimize boundary condition effects. Figure 2 shows the computational domain in conical frustum-shaped rotor, volute, outlet region and hemispherical inlet region. According to the geometry characteristic of the internal flow field of the centrifugal fan, the complex computational domain is subdivided into four regions, which cover the inlet region, the rotor region,

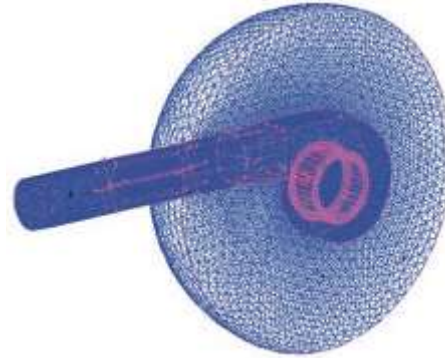


Fig. 3: Retained grid mesh in the three-dimensional model

the volute region and the outlet region. A hybrid structured/ unstructured grid of each region is generated independently in order to ensure the grid's quality, save the computer memory and reduce the computational time. The unstructured grid is used on the radial surfaces, as the shape of the internal flow passage along this direction is very irregular, while the structured grid is used in the axial direction. The interface of neighboring sub-regions consists of identical grid nodes. Figure. 3 shows the grid mesh of the three-dimensional model.

**Experimental Simulation:** Overall measurements have been carried out on the test bench shown in Figure. 4, designed and built at Amikabir University of technology according to the ISO 5801:1997 standard [14]. The standard proposes four arrangements to perform this test. A Pitot-tube is perhaps the simplest device for measuring flow rate at a point. The Pitot tube measures the fluid velocity by converting the kinetic energy of the flow into potential energy. The conversion takes place at the stagnation point, located at the Pitot tube entrance.

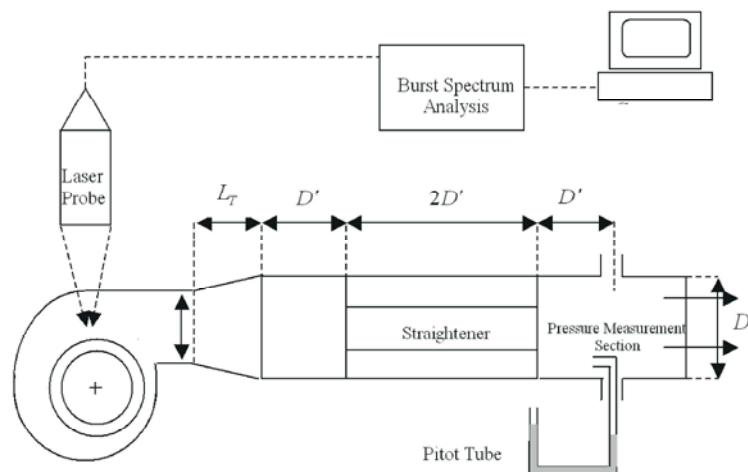


Fig. 4: Sketch of the experimental installation used to determine fan performance and efficiency



Fig. 5: Test bench ISO 5801:1997 of the experimental apparatus

A pressure higher than the free-stream pressure results from the kinematic to potential conversion. This "static" pressure is measured by comparing it to the flow's dynamic pressure with a differential manometer. Static pressure provided by the outflow of centrifugal fan is measured using Pitot tube in channel. It consists of a tube connected at one end to a pressure device such as a manometer and open at the other. To restrain the swirl flow inside the channel, using a Straightener is recommended. The rotational speed is set by a frequency aviator and measured using an optical tachometer of 0.1 % accuracy. The test was performed by 3-phase AC motor with nominal starting torque 2 Kw.

The following are the nominal dimensions of the test bench:

$$0.95 \leq \frac{\pi D'^2}{4Bh} \leq 1.07$$

$$L_T = D' \quad \text{when} \quad B < \frac{4h}{3}$$

$$L_T = \frac{0.75B}{h} \quad \text{when} \quad B > \frac{4h}{3}$$

Velocity measurements in fluid flows are necessary for many important applications. For example, designing turbomachines is an ongoing challenging task. One key aspect for improving the performance of turbomachines is to understand the occurring flow velocity fields inside the machine. Since flow simulation results are either not available or have to be validated, measurements must be conducted during operation at harsh environmental conditions inside the machine. An optical measurement technique Laser Doppler Anemometry LDA is applied (Figure 5). Here, the scattered light signal of a tracer particle is analyzed when it passes an interference fringe system created by two superposed coherent laser beams. The measured frequency of this burst signal equals the Doppler frequency and is directly proportional to one component of the velocity. In case of LDA, two crossing coherent laser beams generate a fringe system with the fringe spacing due to interference.

This system uses a Blue light laser with wavelength 488nm and a Green light laser with wavelength 512.5nm.

Solutions were obtained for a range of flow rates so that fan performance data were generated and compared with the available test data. The following non-dimensional parameters and efficiency equation were used to characterize the fan performance:

$$\text{Flow Coefficient: } \phi = \frac{4q_v}{\pi^2 ND^3}$$

$$\text{Head coefficient: } \psi = \frac{2p_{tf}}{\rho \pi^2 N^2 D^2}$$

$$\text{Efficiency: } \eta = k_p \left( \frac{q_v P_{tf}}{P_R} \right)$$

## RESULTS

It is essential and instructive to choose some particular sections as defined in figures below for the visualization of flow patterns throughout the fan. At first, an analysis of the overall flow field is presented to enhance the physical understanding. Then the numerical results are summarized to yield the effect of shape optimization of rotor. The flow characteristic yielded by the presented simulation results is discussed in the following subsections. Figures. 6, 7 and 8 indicate that the conical frustum-shaped rotor, at the normal range of flow coefficient, has more efficiency than the cylindrical rotor in a similar head coefficient.

**The Velocity Distribution:** Fig. (9-14) show velocity components in sections  $\theta = 270^\circ$  and  $360^\circ$  for conical frustum-shaped and cylindrical rotor and the distributions of velocity contours. The flow is sucked into the fan along the axial direction and then gradually turns into a

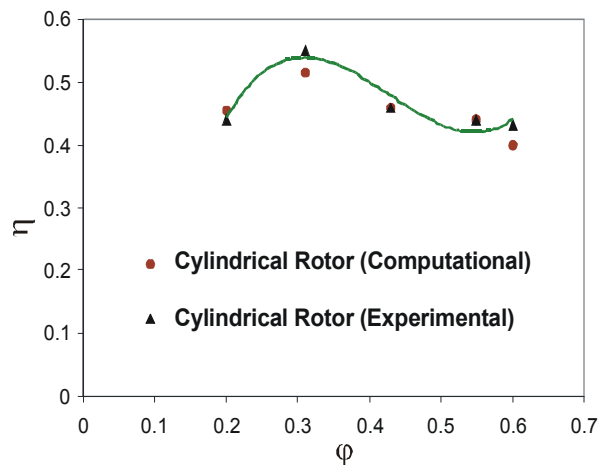


Fig. 6. Flow coefficient versus Head coefficient

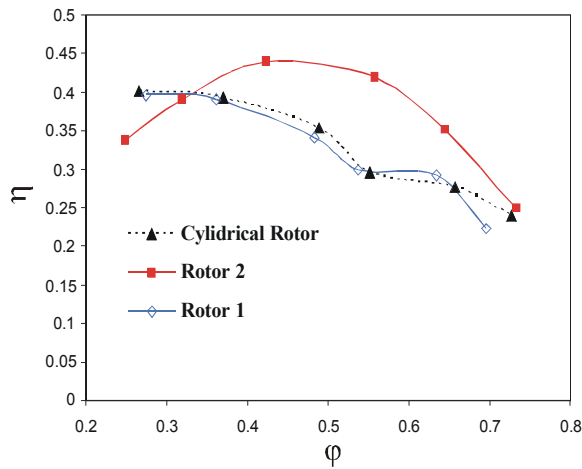


Fig. 7: Flow coefficient versus Efficiency

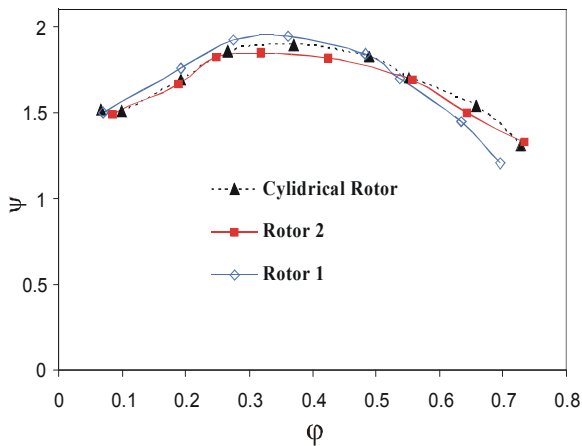


Fig. 8: Flow coefficient versus Head coefficient

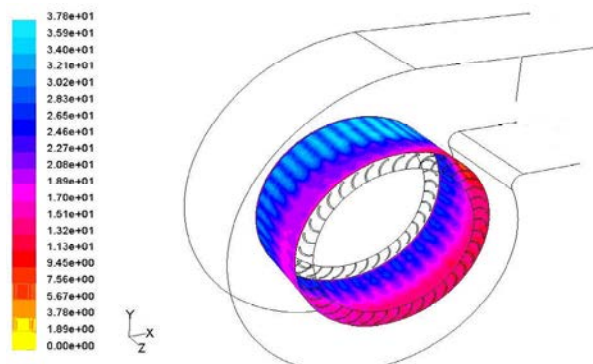


Fig. 9: The results about the distributions of velocity contours

flow along the radial direction near the back plate of the rotor. Thus, the resulting separated flow occurs near the shroud side. Moreover, there is a distinct inactive flow region behind the fan's inlet, as the inlet section is inserted into the top plate of the volute.

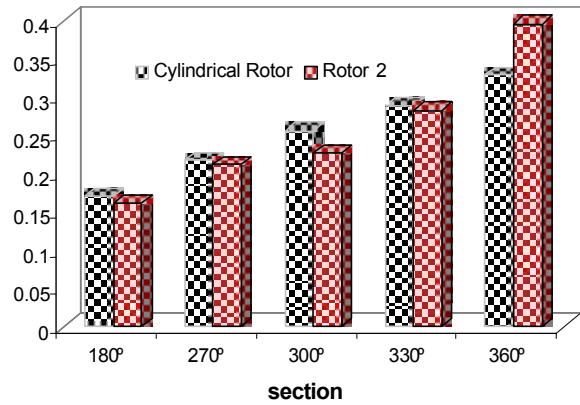


Fig. 10: Mass flow outlet distribution in particular sections

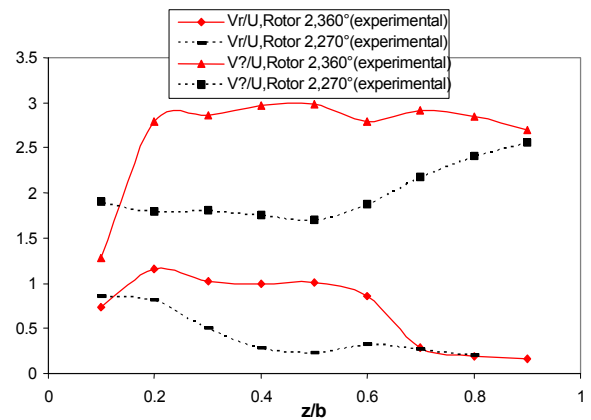


Fig. 11: Velocity components in sections  $\theta = 270^\circ$  and  $360^\circ$

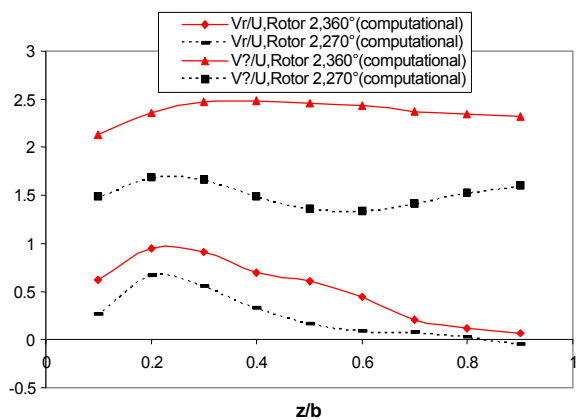


Fig. 12: Velocity components in sections  $\theta = 270^\circ$  and  $360^\circ$

Therefore, in the absence of the front plate, a flow recirculation region emerges by incorporating the separated and inactive flow, which will lead to a non-uniform outflow at the rotor's exit. Our calculations have shown that the flow recirculation can be expressed as a function of circumferential location.

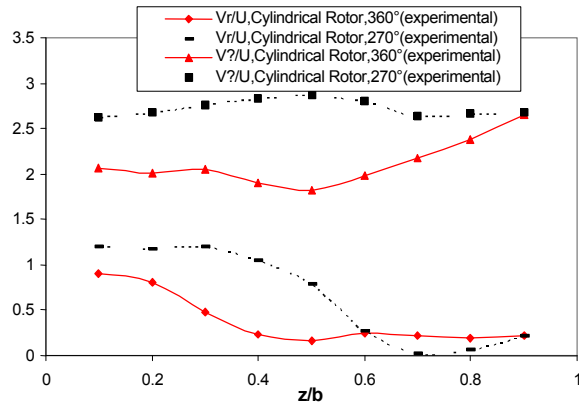


Fig. 13: Velocity components in sections  $\theta = 270^\circ$  and  $360^\circ$

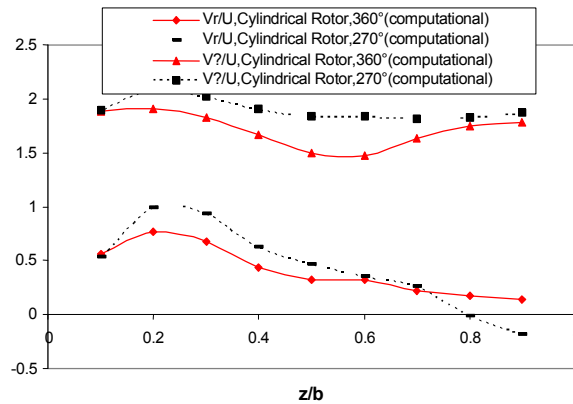


Fig. 14: Velocity components in sections  $\theta = 270^\circ$  and  $360^\circ$

Another notable feature is a small part of the flux entering the rotor, though most of the flux enters the rotor's leading edge, which is due to the inlet's outlet diameter being designed larger than the rotor inlet diameter. It is also related with the circumferential location. Additionally, leakage flow occurs through the gap between the rotating wheel and the fan's inlet after the volute tongue, inevitably causing mixing losses inside the fan. Considering both experimental and numerical results, it is clearly that using the conical rotor (Rotor 2), cause to exit main portion of the flow from section  $\theta = 360^\circ$ , thus, the flow traverses short path to outlet region and possess minimum loss.

**The Jet-Wake Pattern at the Rotor's Exit:** The flow turns from axial to radial after entering the fan. Then, flow recirculation occurs in the region near the shroud side, the area of which is a function of its circumferential location and the through flow rate. Vortex flow has been found to cover most of the flow passages and of the rotor's width, while flow reversal occurs in the blade passages after

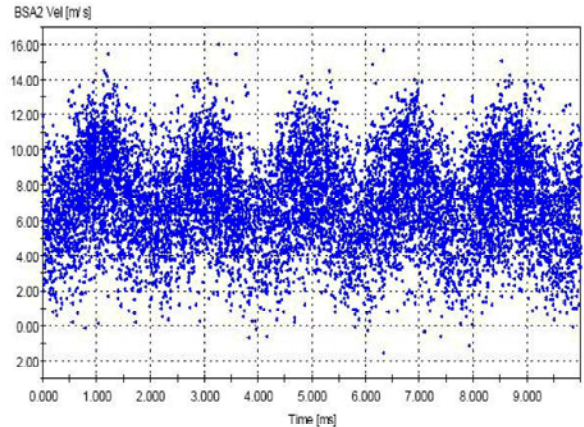


Fig. 15: Velocity fluctuations around rotors (LDA Data)

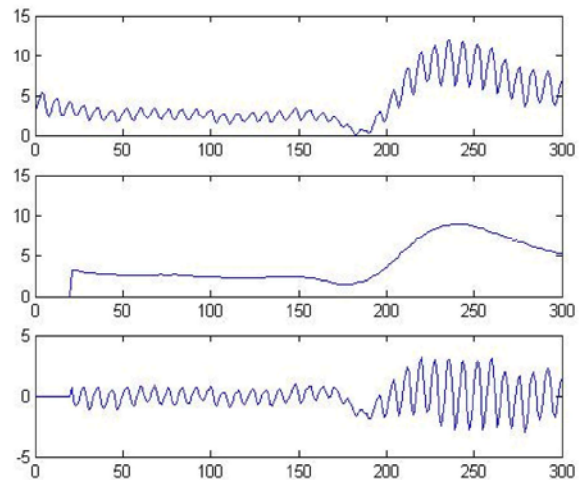


Fig. 16: Velocity fluctuations around rotors

the volute tongue near the shroud side. The jet-wake velocity profile is clearly visible, except for the circumferential area where this flow behavior cannot be easily identified. It is strong in the main flow region and weak in the region opposite to it, due to the high pressure inside the volute. Moreover, it follows that the jet flow is near the pressure surface and the wake flow is near the suction surface. For calculated this flow characteristic the flatness of a distribution is defined as

$$\text{Flatness: } k = \frac{E(x - \mu)^4}{\sigma^4}$$

where  $\mu$  is the mean of  $x$ ,  $\gamma$  is the standard deviation of  $x$  and  $E(t)$  represents the expected value of the quantity  $t$ . flatness is a measure of how outlier-prone a distribution is. The velocity fluctuations shown in Fig. 15 to 18 demonstrate the jet-wake flow have more uniformity in conical rotor; therefore, it makes better mixture flow.

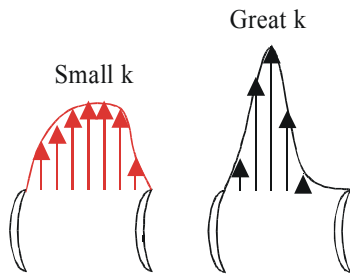


Fig. 17: Exit flow with several magnitude of  $k$

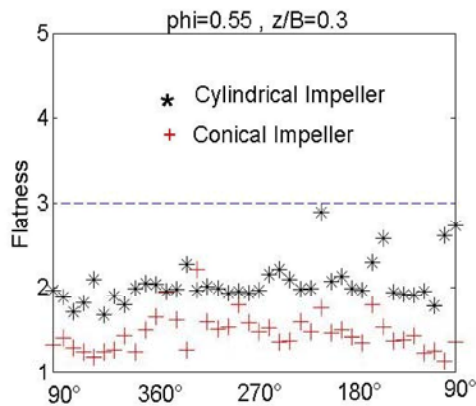


Fig. 18: Flatness magnitude at  $z/B=0.3$

**Concluding Remarks:** Many previous studies have concentrated on the cylindrical rotor of centrifugal fans. In this paper, an experimental test and numerical simulation are carried out to study the performance characteristics of conical frustum-shaped rotor. Different geometries of rotor modifications have been tested. The main objective of this work is to increase performance and efficiency during the whole flow range. Our three-dimensional numerical analysis of the viscous turbulent flow field in a multi-blade centrifugal fan has been implemented successfully. The calculated flow field distribution provides a comprehensive understanding of the overall flow pattern inside the fan. The experimental results matched the numerical predictions, so that the effect of rotor shape optimization on the fan efficiency was acknowledged. There are evident strong three-dimensional characteristics inside the fan when this special geometric configuration is involved. All of these flow features influence the efficiency of the fan.

- Using the conical rotor cause to exit main portion of the flow from section  $\theta = 360^\circ$ , thus, the flow traverses short path to outlet region and possess minimum loss.

- The jet-wake flow has more uniformity in conical rotor; therefore, it cause the air flow to mix better.

Hopefully, the results presented in this paper will contribute much improvements in fan performance. It should be interesting to extend this work by using numerical optimization method to find an optimal rotor-volute matching.

## ACKNOWLEDGEMENT

The authors would like to express their gratitude and thank Amir Kabir University of technology Laboratory for providing experimental resource.

## REFERENCES

1. Raj, D. and W.B. Swim, 1981. Trans ASME, J. Engng., Power, 103(4): 393.
2. Yamazaki, S. and R. Satoh, 1986. Trans. JSME., B52(484): 3987 (in Japanese).
3. Kind, R.J. and M.G. Tobin, 1990. Trans. ASME, J. Turbomach., 112(1): 84.
4. Denger, G.R. and M.W. McBride, 1990. Proc. Fluid Measurement and Instrumentation Forum, ASME, New York, USA, pp: 49-56.
5. Kadota, S., K. Kawaguchi, M. Suzuki, K. Matsui and K. Kikuyama, 1994. Trans. JSME., B60(570): 452 (in Japanese).
6. Kawaguchi, K., S. Kadota, M. Suzuki, K. Matsui and K. Kikuyama, 1994. Trans. JSME., B60(570) 458 (in Japanese).
7. Sandra, V.S., B.T. Rafael, S.M. Carlos and G. Jose, 2001. Trans. ASME, J. Fluids Engng., 123(6): 265.
8. Yamazaki, S. and R. Satoh, 1987. Trans. JSME., B53(485): 108 (in Japanese).
9. Yamazaki, S., R. Satoh and Y. Ohkuma, 1987. Trans. JSME., B53(490): 1730 (in Japanese).
10. Yamazaki, S., K. Hashimoto and Y. Fukasaku, 1996. Trans. JSME., B62(602): 3654 (in Japanese).
11. Yamazaki, S., K. Hashimoto and Y. Fukasaku, 1997. Trans JSME., B63(614): 3325 (in Japanese).
12. Yamamoto, S., F. Kuratani and T. Ogawa, 1999. Trans. JSME., B65(635): 2406 (in Japanese).
13. Fluent 2006. 6.3, Fluent Inc.
14. ISO., 5801. Industrial fans—performance testing using standardized airways, 1993.

Nomenclature

$b$	Rotor Width	$h$	Exit throttle High	$V_r$	Radial Velocity
$B$	Volute Width	$L_B$	Length of Reversal Flow	$v_\theta$	Tangential Velocity
$\alpha$	Rotor Angle	$L_T$	Flexible Connector Length	$U$	Rotor linear velocity
$r$	Volute Expansion radius	$\gamma$	Volute Expansion Angle	$\eta$	Efficiency
$n$	Number of Blade	$\alpha$	the standard deviation of x	$P_R$	Input Power
$N$	Revolutions per Minute	$D_s$	Exit Channel Diameter	$q_m$	Mass Flow Rate
$D_1$	Inlet Diameter of Rotor	$\phi$	Flow Coefficient	$P_a$	Atmosphere Pressure
$D_2$	Outlet Diameter of Rotor	$\psi$	Head coefficient	$z$	Distance from Back Wall of Volute
$D$	Average Diameter of Rotor	$q_v$	Volume Flow Rate	$\mu$	The mean of x
$\beta_1$	Inlet Angle ( blade )	$P_{tf}$	Fan Total Pressure	$E(t)$	The expected value of the quantity $t$
$\beta_2$	Outlet Angle ( blade )	$\rho$	Air Density		